Participation of (η^3-Allyl)ruthenium(II) Complexes in C−C Bond Formation and C−C Bond Cleavage. A Theoretical Study

Shigeyoshi Sakaki,*,† Tetsuro Ohki,† Tatsunori Takayama,† Manabu Sugimoto,† Teruyuki Kondo,‡ and Take-aki Mitsudo‡

Department of Applied Chemistry and Biochemistry, Faculty of Engineering, Kumamoto University, Kurokami, Kumamoto 860-8555, Japan, and Department of Energy and Hydrocarbon Chemistry, Graduate School of Engineering, Kyoto University, Sakyo-ku, Kyoto 606-8501, Japan

Received January 3, 2001

Coupling reactions of formaldehyde with RuBr(η^3-C_3H_5)$(CO)_3$ (**R1**), [Ru(η^3-C_3H_5)(HCHO)$(CO)_3$]$^+$ (**I2**), and RuBr(η^3-C_3H_5)(HCHO)$(CO)_2$ (**I3**) were theoretically investigated with ab initio MP2-MP4(SDQ), CCSD(T), and DFT(B3LYP) methods. In **R1**, the coupling reaction takes place through two transition states, as follows: coordination of formaldehyde with the ruthenium(II) center occurs through the first transition state, to afford an (η^1-allyl)ruthenium(II) formaldehyde complex, RuBr(η^1-C_3H_5)(HCHO)$(CO)_3$, as an intermediate, and then C−C bond formation between the η^1-allyl ligand and formaldehyde takes place through the second transition state, to afford RuBr($OCH_2CH_2CH{=}CH_2$)$(CO)_3$. The activation energy (E_a) is 19.9 (12.0) kcal/mol for the first transition state and 12.5 (5.4) kcal/mol for the second transition state, where the values given without parentheses are E_a values calculated with the MP4(SDQ) method and the values in parentheses are those calculated with the DFT method. In **I2** and **I3**, the coupling reaction proceeds through one transition state, to afford [Ru($OCH_2CH_2CH{=}CH_2$)$(CO)_3$]$^+$ and RuBr($OCH_2CH_2CH{=}CH_2$)$(CO)_2$ with considerably larger E_a values of 50.7 (30.6) and 34.8 (32.0) kcal/mol, respectively. Even in **I2**, however, the allyl−aldehyde coupling reaction easily occurs through two transition states like that of **R1**, when one more formaldehyde molecule coordinates with the ruthenium(II) center; the E_a value is 10.5 (4.6) kcal/mol for the first transition state and 13.6 (6.7) kcal/mol for the second transition state. In this case, one formaldehyde molecule plays the role of a spectator ligand and the second formaldehyde undergoes a coupling reaction with the allyl ligand. From these results, it should be concluded that the allyl−aldehyde coupling reaction proceeds easily in the coordinatively saturated (η^3-allyl)ruthenium(II) complex and that the coordinatively unsaturated (η^3-allyl)ruthenium(II) complex becomes reactive when two molecules of formaldehyde coordinate with the ruthenium(II) center. IRC calculation of the allyl−aldehyde coupling reaction of **R1** clearly shows that the C−C bond formation between the η^1-allyl ligand and formaldehyde occurs after the second transition state concomitantly with the bond alternation in the η^1-allyl ligand. Electron redistribution in the reaction indicates that the allyl−aldehyde coupling reaction is understood in terms of electrophilic attack of formaldehyde to the allyl ligand. Reverse C−C bond cleavage proceeds with a moderate E_a value of 16.6 (13.5) kcal/mol in [Ru($OCH_2CH_2CH{=}CH_2$)$(CO)_3$]$^+$ to afford [Ru(η^3-C_3H_5)(HCHO)$(CO)_3$]$^+$, with a similar E_a value of 19.6 (11.1) kcal/mol in RuBr($OCH_2CH_2CH{=}CH_2$)$(CO)_3$ to afford RuBr(η^3-C_3H_5)$(CO)_3$ + HCHO, and with a considerably large E_a value of 27.0 (26.8) kcal/mol in RuBr($OCH_2CH_2CH{=}CH_2$)$(CO)_2$ to afford RuBr(η^3-C_3H_5)(HCHO)$(CO)_2$. [Ru($OCH_2CH_2CH{=}CH_2$)$(CO)_3$]$^+$ is the best for this C−C bond cleavage. This is because the coordinatively unsaturated complex with electron-accepting ligands yields a stable (η^3-allyl)ruthenium(II) complex in which the η^3-allyl ligand is strongly electron donating and needs two coordination sites. Though the C−C bond cleavage of RuBr($OCH_2CH_2CH{=}CH_2$)$(CO)_3$ occurs with a moderate E_a value, this reaction is much less exothermic than that of [Ru($OCH_2CH_2CH{=}CH_2$)$(CO)_3$]$^+$.

Introduction

η^3-Allyl transition-metal complexes have attracted considerable interest, since they are used in various synthetic reactions as a catalyst.[1] One of their useful and interesting reactions is C−C bond formation. The C−C bond formation is carried out in general by nucleophilic attack of a carbanion at an η^3-allyl ligand coordinated with a transition-metal complex,[1−3] η^3-allyl−alkyl and η^3-allyl−aryl reductive eliminations of

† Kumamoto University.
‡ Kyoto University.

10.1021/om010011g CCC: $20.00
Publication on Web 06/15/2001

η^3-allyl transition-metal complexes,[1,4] and coupling reactions of aldehyde and ketone with η^3-allyl and η^1-allyl transition-metal complexes.[1,5−14] C−C bond cleavage under homogeneous conditions is also one of the challenging subjects of recent research.[15] Many attempts have been made to perform C−C bond cleavage by utilizing the release of ring strain energy,[16] the attainment of aromaticity,[17] the intramolecular proximity of the C−C bond to the metal,[18] and the carbonyl functionality which is due to the weak C−C bond between carbonyl carbon and α-carbon atoms and the formation of a stable metal−C(O)R bond.[19] Besides these methods, formation of a stable η^3-allyl transition-metal complex was also utilized for the C−C bond cleavage. For instance, the C−C bond cleavage was achieved with palladium(II) complexes by formation of their η^3-allyl complexes.[20] This reaction is regarded as the reverse reaction of the nucleophilic attack of a carbanion at the η^3-allyl ligand. Similar C−C bond cleavage was reported in ruthenium(II) complexes, in which the β-methyl group of ruthenacyclobutane was transferred to the ruthenium(II) center to afford an (η^3-allyl)ruthenium-(II) complex.[21] Recently, the catalytic C−C bond cleavage of homoallyl alcohols was carried out with ruthenium(II) complexes to afford propene and ketone,[22] which was regarded as the reverse of an allyl−ketone coupling reaction. In these reactions, formation of the stable η^3-allyl transition-metal complex is considered as an important driving force. Thus, it is of considerable interest to clarify the coordinate bonding nature, electronic structure, and reactivity, as well as the stability, of η^3-allyl transition-metal complexes.

Many theoretical works with molecular orbital and DFT methods have been reported on geometries of η^3-allyl transition-metal complexes,[23−25] nucleophilic attack at the η^3-allyl ligand coordinated with palladium(II) complexes,[26−30] and reductive eliminations of the η^3-allyl

(1) For instance: (a) Trost, B. M.; Verhoeven, T. R. In *Comprehensive Organometallic Chemistry*; Wilkinson, G., Stone, F. G. A., Abel, E. W., Eds.; Pergamon Press: Oxford, U.K., 1982; Vol. 8, p 799. (b) Collman, J. P.; Hegedus, L. S.; Norton, J. R.; Finke, R. G. *Principles and Applications of Organotransition Metal Chemistry*; University Science Books: Mill Valley, CA, 1987; pp 175, 417, 881. (c) Hegedus, L. S. *Transition Metals in the Synthesis of Complex Organic Molecules*; University Science Books; Mill Valley, CA, 1994; p 261. (d) Trost, B. M. *Acc. Chem. Res.* **1996**, *29*, 355.

(2) For instance: (a) Trost, B. M.; Bunt, R. C. *J. Am. Chem. Soc.* **1994**, *116*, 4089; **1998**, *120*, 70. (b) Chang, S.; Yoon, J.; Brookhart, M. *J. Am. Chem. Soc.* **1994**, *116*, 1869.

(3) (a) Zhang, S.-W.; Mistudo, T.; Kondo, T.; Watanabe, Y. *J. Organomet. Chem.* **1993**, *450*, 197. (b) Kondo, T.; Ono, H.; Satake, N.; Mitsudo, T.; Watanabe, Y. *Organometallics* **1995**, *14*, 1945. (c) Morisaki, Y.; Kondo, T.; Mitsudo, T. *Organometallics* **1999**, *18*, 4722.

(4) (a) Kurosawa, H.; Emoto, M.; Ohnishi, H.; Miki, K.; Kasai, N.; Tatsumi, K.; Nakamura, A. *J. Am. Chem. Soc.* **1987**, *109*, 6333. (b) Kurosawa, H.; Ohnishi, H.; Emoto, M.; Chatani, N.; Kawasaki, Y.; Murai, S.; Ikeda, I. *Organometallics* **1990**, *9*, 3038. (c) Trost, B. M.; Flygare, J. A. *J. Am. Chem. Soc.* **1992**, *114*, 5476.

(5) Corey, E. J.; Semmelhack, M. F. *J. Am. Chem. Soc.* **1967**, *89*, 2755.

(6) Hegedus, L. S.; Wagner, S. D.; Waterman, E. L.; Siirala-Hansen, K. *J. Org. Chem.* **1975**, *40*, 593.

(7) Matsubara, S.; Wakamatsu, K.; Morizawa, Y.; Tsuboniwa, N.; Oshima, K.; Nozaki, H. *Bull. Chem. Soc. Jpn.* **1985**, *58*, 1196.

(8) Tabuchi, T.; Inanaga, J.; Yamaguchi, M. *Tetrahedron Lett.* **1986**, *27*, 1195.

(9) Collins, S.; Dean, W. P.; Ward, D. G. *Organometallics* **1988**, *7*, 2289.

(10) (a) Masuyama, Y.; Takahara, J. P.; Kurusu, Y. *J. Am. Chem. Soc.* **1988**, *110*, 4473. (b) Takahara, J. P.; Masuyama, Y.; Kurusu, Y. *J. Am. Chem. Soc.* **1992**, *114*, 2577.

(11) Faller, J. W.; Linebarrier, D. L. *J. Am. Chem. Soc.* **1989**, *111*, 1937.

(12) Hafner, A.; Duthaler, R. O.; Marti, R.; Rihs, G.; Rothe-Streit, P.; Schwarzenbach, F. *J. Am. Chem. Soc.* **1992**, *114*, 2321.

(13) (a) Ohno, K.; Tsuji, J. *Chem. Commun.* **1971**, 247. (b) Nakamura, H.; Asao, N.; Yamamoto, Y. *J. Chem. Soc., Chem. Commun.* **1995**, 1273. (c) Nakamura, H.; Iwama, H.; Yamamoto, Y. *J. Am. Chem. Soc.* **1996**, *118*, 6641.

(14) (a) Maruyama, Y.; Shimizu, I.; Yamamoto, A. *Chem. Lett.* **1994**, 1041. (b) Komiya, S.; Kabasawa, T.; Yamashita, K.; Hirano, M.; Fukuoka, A. *J. Organomet. Chem.* **1994**, *471*, C6. (c) Tlanas, T. G.: Marumo, T.; Ichikawa, Y.; Hirano, M.; Komiya, S. *J. Mol. Catal. A* **1999**, *147*, 137.

(15) (a) Collman, J. P.; Hegedus, L. S.; Norton, J. R.; Finke, R. G. *Principles and Applications of Organotransition Metal Chemistry*; University Science Books: Mill Valley, CA, 1987; p 305. (b) Rybtchinski, B.; Milstein, D. *Angew. Chem., Int. Ed.* **1999**, *38*, 870. (c) Murakami, M.; Ito, Y. In *Activation of Unreactive Bonds and Organic Synthesis*; Murai, S., Ed.; Springer: New York, 1999; p 97. (d) Kondo, T.; Mitsudo, T. *J. Synth. Org. Chem. Jpn.* **1999**, *57*, 552. (e) Mitsudo, T.; Kondo, T. *Synlett*, in press.

(16) (a) Adams, D. M.; Chatt, J.; Guys, R. G.; Sheppard, N. *J. Chem. Soc.* **1961**, 738. (b) Bailey, N. A.; Gillard, R. D.; Keeton, M.; Mason, R.; Russell, D. R. *J. Chem. Soc., Chem. Commun.* **1966**, 396. (c) McQuillin, F. J.; Powell, K. C. *J. Chem. Soc., Dalton Trans.* **1972**, 2123. (d) Barretta, A.; Cloke, F. G. N.; Feigenbaum, A.; Green, M. L. H.; Gourdon, A.; Prout, K. *J. Chem. Soc., Chem. Commun.* **1981**, 156. (e) Barretta, A.; Chong, K. S.; Cloke, F. G. N.; Feigenbaum, A.; Green, M. L. H. *J. Chem. Soc., Dalton Trans.* **1983**, 861. (f) Flood, T. C.; Statler, J. A. *Organometallics* **1984**, *3*, 1795. (g) Eisch, J. J.; Piotrowski, A. M.; Han, K. I.; Krüger, C.; Tsay, Y. H. *Oraganometallics* **1985**, *4*, 4. (h) Schwager, H.; Spyroudis, S.; Vollhardt, K. P. C. *J. Organomet. Chem.* **1990**, *382*, 191. (i) Lu, Z.; Jun, C.-H.; de Gala, S. R.; Sigalas, M.; Eisenstein, O.; Crabtree, R. H. *J. Chem. Soc., Chem. Commun.* **1993**, 1877. (j) Lu, Z.; Jun, C.-H. de Gala, S. R.; Eisenstein, O.; Crabtree, R. H. *Organometallics* **1995**, *14*, 1168. (k) Perthuisot, C.; Edelbach, B. E.; Zubris, D. L.; Jones, W. D. *Organometallics* **1997**, *16*, 2016. (l) Shaltout, R. M.; Sygula, R.; Sygula, A.; Fronczek, F. R.; Stanley, G. G.; Rabideau, P. W. *J. Am. Chem. Soc.* **1997**, *120*, 8835. (m) Edelbach, B. L.; Vicic, D. A.; Lachicotte, R. J.; Jones, W. D. *Organometallics* **1998**, *17*, 4784. (n) Edelbach, B. L.; Vicic, D. A.; Lachicotte, R. J.; Jones, W. D. *J. Am. Chem. Soc.* **1998**, *120*, 2843.

(17) (a) Kang, J. W.; Moseley, K.; Maitlis, P. J. *J. Am. Chem. Soc.* **1969**, *91*, 5970. (b) Benfield, F. W.; Green, M. L. H. *J. Chem. Soc., Dalton Trans.* **1974**, 1324. (c) Eilbracht, P. *Chem. Ber.* **1976**, *109*, 1429. (d) Crabtree, R. H.; Dion, R. P.; Gibboni, D. J.; McGrath, D. V.; Holt, E. M. *J. Am. Chem. Soc.* **1986**, *108*, 7222. (e) Hemond, R. C.; Hughes, R. P.; Locker, H. B. *Organometallics* **1986**, *5*, 2391. (f) Jones, W. D.; Maguire, J. A. *Organometallics* **1987**, *6*, 1301.

(18) (a) Suggs, J. W.; Jun, C.-H. *J. Chem. Soc., Chem. Commun.* **1985**, 92. (b) Gozin, M.; Weisman, A.; Ben-David. Y.; Milstein, D. *Nature* **1993**, *364*, 699. (c) Gozin, M.; Aizenberg, M.; Liou, S.-Y.; Weisman, A.; Ben-David, Y.; Milstein, D. *Nature* **1994**, *370*, 42. (d) Liou, S.-Y.; Gozin, M.; Milstein, D. *J. Chem. Soc., Chem. Commun.* **1995**, 1165. (e) Liou, S.-Y.; Gozin, M.; Milstein, D. *J. Am. Chem. Soc.* **1995**, *117*, 9774. (f) Rybtchinski, B.; Vigalok, A.; Ben-David, Y.; Milstein, D. *J. Am. Chem. Soc.* **1996**, *118*, 12406. (g) van der Boom, M. E.; Kraatz, H.-B.; Ben-David, Y.; Milstein, D. *J. Chem. Soc., Chem. Commun.* **1996**, 2167. (h) Liou, S.-Y.; van der Boom, M. E.; Maitlis, D. *Chem. Commun.* **1998**, 687. (i) Gandelman, M.; Vigalok, A.; Shimon, L. J. W.; Milstein, D. *Organometallics* **1997**, *16*, 3981. (j) Rybtchinski, B.; Milstein, D. *J. Am. Chem. Soc.* **1999**, *121*, 4528.

(19) (a) Rusina, A.; Vlcek, A. A. *Nature* **1965**, *206*, 295. (b) Wong, W.; Singer, S. J.; Pitts, W. D.; Watkins, S. F.; Baddley, W. H. *J. Chem. Soc., Chem. Commun.* **1972**, 672. (c) Visser, J. P.; Ramakers-Blom, J. E. *J. Organomet. Chem.* **1972**, *44*, C63. (d) Song, L.; Arif, A. M.; Stang, P. J. *Organometallics* **1990**, *9*, 2792. (e) Evans, J. A.; Everitt, G. F.; Kemmitt, R. D. W.; Russell, D. R. *J. Chem. Soc., Chem. Commun.* **1973**, 158. (f) Hammer, E. R.; Kemmitt, R. D. W.; Smith, M. A. R. *J. Chem. Soc., Chem. Commun.* **1974**, 841. (g) Liebeskind, L. S.; Baysdon, S. L.; South, M. S. *J. Organomet. Chem.* **1980**, *202*, C73. (h) Liebeskind, L. S.; Baysdon, S. L.; South, M. S.; Iyer, S.; Leeds, J. P. *Tetrahedron* **1985**, *41*, 5839. (i) Huffman, M. A.; Liebeskind, L. S.; Pennington, W. T. *Organometallics* **1992**, *11*, 255. (j) Suggs, J. W.; Jun, C. H. *J. Am. Chem. Soc.* **1984**, *106*, 3054; **1986**, *108*, 4679. (k) Jun, C. H.; Kang, J. B.; Lim, Y. G. *Tetrahedron Lett.* **1995**, *36*, 277. (l) Suggs, J. W.; Wovkulich, M. J.; Cox, S. D. *Organometallics* **1985**, *4*, 1101. (m) Murakami, M.; Amii, H.; Ito, Y. *Nature* **1994**, *370*, 540. (n) Murakami, M.; Amii, H.; Shigeto, K.; Ito, Y. *J. Am. Chem. Soc.* **1996**, *118*, 8285.

(20) Nilsson, Y. I. M.; Andersson, P. G.; Bäckvall, J.-E. *J. Am. Chem. Soc.* **1993**, *115*, 6609.

(21) McNeill, K.; Anderson, R. A.; Bergman, R. G. *J. Am. Chem. Soc.* **1995**, *117*, 3625; **1997**, *119*, 11244.

(22) Kondo, T.; Kodoi, K.; Nishinaga, E.; Okada, T.; Morisaki, Y.; Watanabe, Y.; Mitsudo, T. *J. Am. Chem. Soc.* **1998**, *120*, 5587.

(23) Nakatsuji, K.; Yamaguchi, M.; Tatsumi, I.; Nakamura, A. *Organometallics* **1984**, *3*, 1257.

(24) Goddard, R.; Krueger, C.; Mark, F.; Stansfield, R.; Zhang, X. *Organometallics* **1985**, *4*, 285.

(25) Szabo, K. J. *J. Am. Chem. Soc.* **1996**, *118*, 7818.

Scheme 1

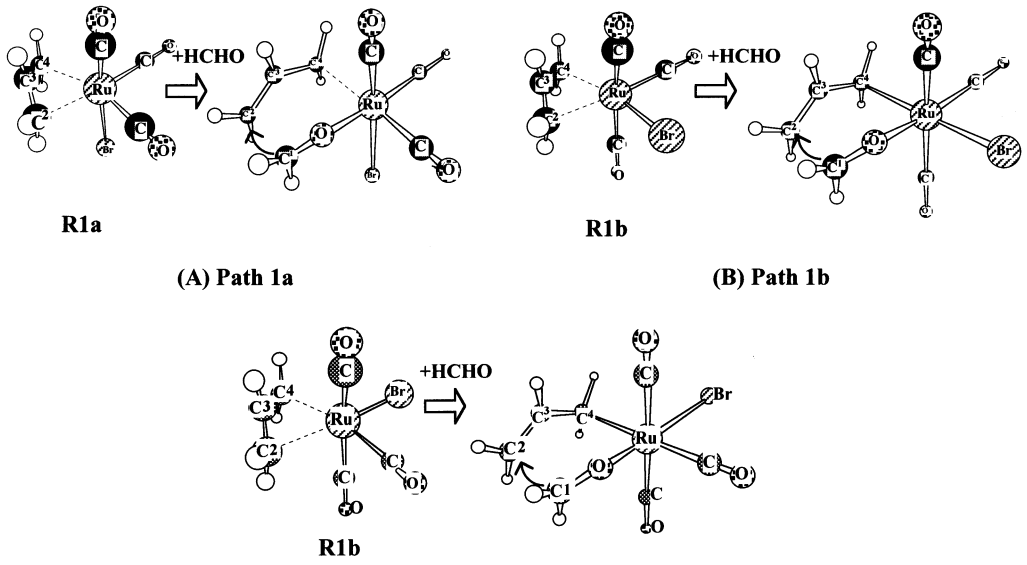

ligand with H (hydride), methyl, silyl, and similar groups.[31] However, no theoretical work has been carried out on the coupling reactions of aldehyde and ketone with the η^3-allyl ligand of transition-metal complexes, except for recent pioneering works concerning the reactions of (η^3-allyl)palladium(II) complex with ketone and imine.[32] Sufficient information has not been presented on the reaction features, including the transition state structure, geometry changes, and electronic process. To understand well the coupling reaction and the C−C bond cleavage and to achieve new development in these reactions, a detailed investigation of the aforementioned issues is indispensable.

In this work, we have theoretically investigated the coupling reaction of formaldehyde with (η^3-allyl)ruthenium(II) complexes and the reverse C−C bond cleavage of ruthenium(II) homoallyl−alkoxide complexes. We selected here the ruthenium(II) complexes, since the (η^3-allyl)ruthenium(II) complex participates in both the allyl−aldehyde coupling reaction[3a,b] and the C−C bond cleavage.[22] Also, no theoretical work has been reported on the (η^3-allyl)ruthenium(II) complex, to our knowledge. Our purposes here are to present clear answers to the aforementioned issues, to clarify the electronic process of the reaction, and to propose guidelines which are useful to predict good ruthenium complexes for the allyl−aldehyde coupling reaction and the C−C bond cleavage.

Models of Reaction System

Since ruthenium(II) takes a d^6 electron configuration, a six-coordinate complex is coordinatively saturated. Actually, six-coordinate ruthenium(II) complexes such as $RuX(\eta^3\text{-}C_3H_5)(CO)_3$ (X = Cl,[33] Br,[33] AcO,[3b] OTf[3b]) are experimentally known, where the η^3-allyl ligand is considered to occupy two coordination sites. Since these complexes undergo the allyl−aldehyde coupling reaction, we theoretically investigated the reaction of formaldehyde with $RuBr(\eta^3\text{-}C_3H_5)(CO)_3$ (**R1**), where formaldehyde was adopted as the simplest model for carbonyl compounds. There are two possible molecular structures in **R1**, such as a facial structure (**R1a**) and a meridional one (**R1b**), as shown in Scheme 1. In the facial complex **R1a**, Br takes a position trans to CO. In the meridional species **R1b**, Br is at a position trans to the η^3-allyl ligand. In **R1a**, the exo form of the allyl moiety is slightly less stable than the endo form by 1.7 kcal/mol (MP4(SDQ)/BS-II//HF/BS-I; see Computational Details for the method). Actually, the ratio of endo form to exo form was experimentally reported to be about 40/1.[3b,34,35] Also, **R1a** was considerably more stable than **R1b** by 13.0 kcal/mol (MP4(SDQ)/BS-II//HF/BS-I), where the endo form was taken for the allyl moiety. This is consistent with the experimental result that a facial structure such as **R1a** is experimentally observed in the similar (η^3-allyl)ruthenium(II)[3b,34] and (η^3-allyl)iron(II) complexes.[36] Hence, we investigated the coupling reaction of **R1a** in detail and briefly investigated only the important intermediate, transition state, and product in the coupling reaction of **R1b**, where we adopted the endo form of the allyl ligand in both complexes.

Since OTf^- is a weak ligand, it would easily dissociate from the ruthenium(II) center in $Ru(OTf)(\eta^3\text{-}C_3H_5)(CO)_3$.[3b] The resultant complex, $[Ru(\eta^3\text{-}C_3H_5)(CO)_3]^+$ (**R2**), is coordinatively unsaturated, with which aldehyde can easily coordinate. Thus, one can expect that the allyl−aldehyde coupling reaction would easily occur in **R2**. In **R2**, there are two isomers, as shown in Scheme

(26) Sakaki, S.; Nishikawa, M.; Ohyoshi, A. *J. Am. Chem. Soc.* **1980**, *102*, 4062.
(27) Curtis, M. D.; Eisenstein, O. *Organometallics* **1984**, *3*, 887.
(28) Ward, T. R. *Organometallics* **1996**, *15*, 2836.
(29) Aranyos, A.; Szabo, K. J.; Castano, A. M.; Bäckvall, J.-E. *Organometallics* **1997**, *16*, 1058.
(30) Szabo, K. J.; Hupe, E.; Larsson, A. L. E. *Organometallics* **1997**, *16*, 3779.
(31) (a) Sakaki, S.; Satoh, H.; Shono, H.; Ujino, Y. *Organometallics* **1996**, *15*, 1713. (b) Biswas, B.; Sugimoto, M.; Sakaki, S. *Organometallics* **1999**, *18*, 4015.
(32) (a) Szabo, K. J. *Eur. J. Chem.* **2000**, *6*, 4413. (b) Solin, N.; Narayan, S.; Szabo, K. J. *J. Org. Chem.*, in press.
(33) Sbrana, G.; Braca, G.; Piacenti, F.; Pino, P. *J. Organomet. Chem.* **1968**, *13*, 240.
(34) Wuu, Y.-M.; Wrighton, M. S. *Organometallics* **1988**, *7*, 1839.
(35) The ratio of 40/1 leads to the energy difference between endo and exoo forms of about 9 kcal/mol. The present MP4(SDQ)/BS-II//HF/BS-I calculation considerably underestimated the energy difference.
(36) Simon, F. E.; Lauher, J. W. *Inorg. Chem.* **1980**, *19*, 2338.

Scheme 2

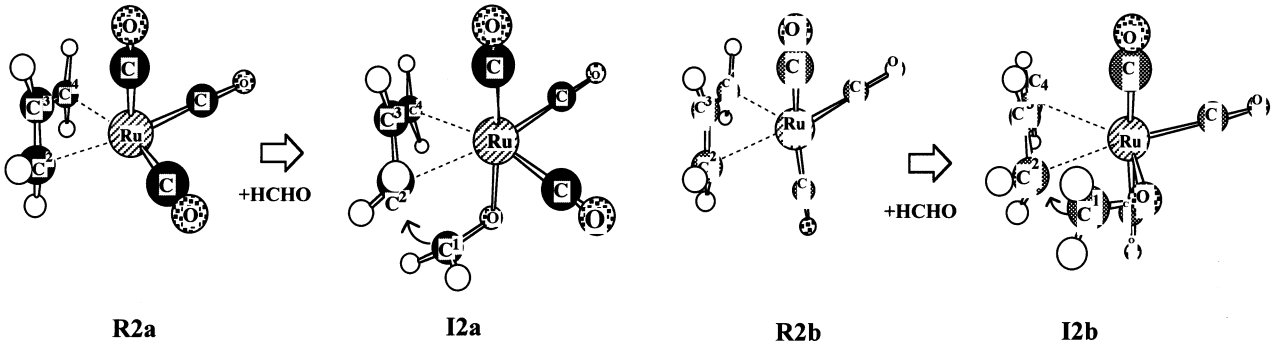

R2a **I2a** **R2b** **I2b**

(A) Path 2a **(B) Path 2b**

Scheme 3

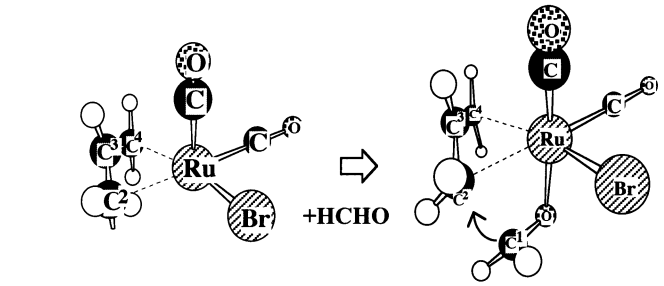

R3a **I3a**

(A) Path 3a

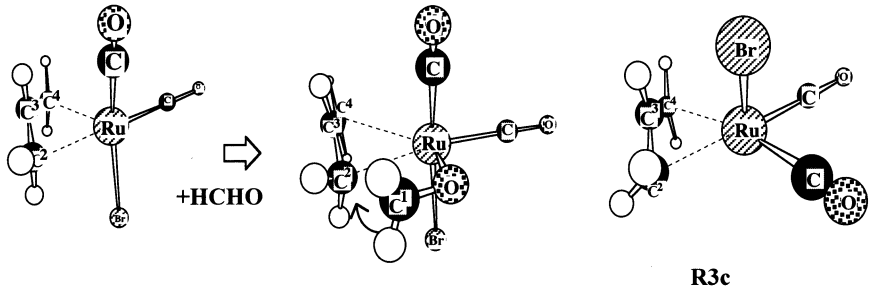

R3b **I3b** **R3c**

(B) Path 3b

2; one (**R2a**) takes a facial structure, and the other (**R2b**) takes a meridional one. The near-UV-light irradiation would induce CO dissociation from **R1**,[34] to afford $RuBr(\eta^3\text{-}C_3H_5)(CO)_2$ (**R3**), which is coordinatively unsaturated as well. In **R3**, there are three isomers, as shown in Scheme 3. However, we excluded one isomer (**R3c**) from our investigation, since this complex is much less stable than **R3a** by 17 kcal/mol (DFT/BS-III). Because of the coordinatively unsaturated structures of **R2a**, **R2b**, **R3a**, and **R3b**, formaldehyde easily coordinates with the ruthenium(II) center, to afford **I2a**, **I2b**, **I3a**, and **I3b**, respectively, as shown in Schemes 2 and 3. The main purpose of this work is to investigate the allyl−aldehyde coupling reaction. Hence, we did not optimize **R2a**, **R2b**, **R3a**, and **R3b** but investigated the allyl−aldehyde coupling reactions starting from **I2a**, **I2b**, **I3a**, and **I3b**, as well as those of **R1a** and **R1b**, where we adopted the endo form of the η^3-allyl moiety to compare these complexes with **R1a**, which is the best complex for the allyl−aldehyde coupling reaction, as discussed below. Theoretical analyses were also performed on the C−C bond cleavage of $RuBr(OCH_2CH_2CH{=}CH_2)(CO)_3$, $[Ru(OCH_2CH_2CH{=}CH_2)(CO)_2]^+$, and $RuBr(OCH_2CH_2CH{=}CH_2)(CO)_2$.

Computational Details

First, we carried out a preliminary investigation, as follows: geometries of reactant, transition state, and product were optimized at the SCF level. The transition state was determined so that the Hessian matrix has only one negative eigenvalue. Important transition states were ascertained with calculations of vibrational frequency. The activation barrier (E_a) and reaction energy (ΔE) were evaluated with the MP4(SDQ) method, where the SCF-optimized geometries were adopted.

Two kinds of basis set systems were used in the preliminary investigation. In both basis set systems, core electrons of Ru (up to 3d) and Br (up to 3d) were replaced with effective core potentials (ECPs).[37,38] In the smaller basis set system (BS-I),

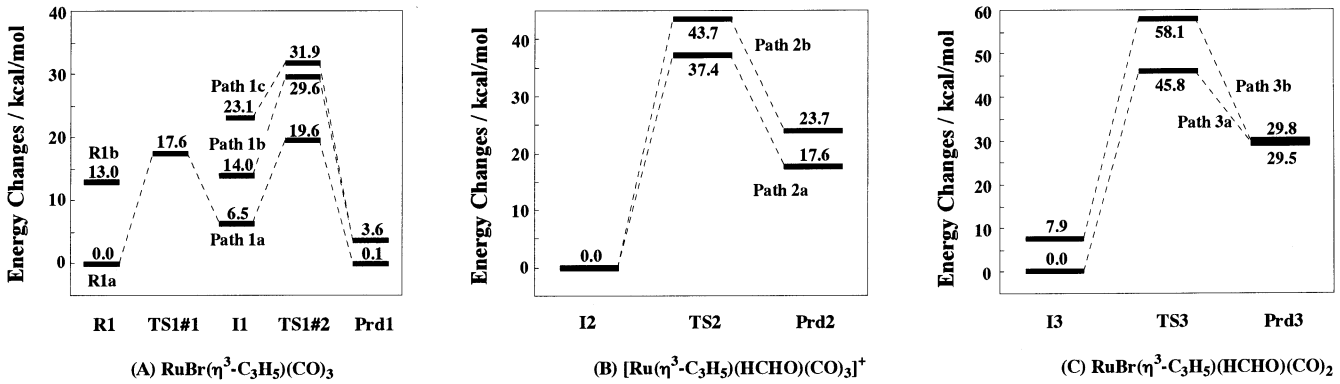

Figure 1. Energy changes (MP4(SDQ)/BS-II//HF/BS-I; in units of kcal/mol) in the allyl−aldehyde coupling reactions with RuBr(η^3-C_3H_5)$(CO)_3$ (**R1**), [Ru(η^3-C_3H_5)$(HCHO)(CO)_3]^+$ (**I2**), and RuBr(η^3-C_3H_5)$(HCHO)(CO)_2$ (**I3**).

valence electrons of Ru and Br were represented with (311/311/31)[37] and (21/21) sets,[38] respectively. For C, O, and H atoms, MIDI-3[39] and (31)[40] sets were employed, respectively. This BS-I system was used for geometry optimization, and results are given in the Supporting Information. In the larger basis set system (BS-II), a slightly more flexible (311/311/211) set was used for valence electrons of Ru with the same ECPs[37] as those of BS-I. For Br, the same basis set and the same ECPs[38] as those of BS-I were employed. Huzinaga−Dunning (721/41) basis sets[40] were used for C and O, where a d-polarization function was added to C and O of the allyl and formaldehyde moieties. These MP4(SDQ)/BS-II//HF/BS-I and HF/BS-I methods are used in Figures 1 and 6.

The preliminary investigation showed that **R1a** was the best complex for the coupling reaction and that the coupling reactions in **I2a** and **I3a** occurred with lower activation energies than those of **I2b** and **I3b**, respectively. Hence, we investigated the reactions of **R1a**, **I2a**, and **I3a** in more detail. Better basis set systems (BS-III and BS-IV) were employed in the detailed investigation. In the BS-III system, 6-31G* set[41] was used for allyl and formaldehyde moieties, while a 6-31G set[41a] was employed for CO. For the other atoms, the same basis sets and ECPs as those of BS-II were employed. Geometries of the reactant, transition state, and product were reoptimized with the DFT/BS-III method in the reactions of **R1a** and **I2a**, where the B3LYP functional[42,43] was adopted for an exchange-correlation term. In the reaction of **I3a**, geometry optimization was carried out with both DFT/BS-III and MP2/BS-III methods, since the DFT/BS-III method provided a strange transition state structure, as discussed below. The E_a and ΔE values were evaluated with DFT and MP4(SDQ) methods, where DFT/BS-III optimized geometries were adopted in the reactions of **R1a** and **I2a** but MP2/BS-III optimized ones were adopted in the reaction of **I3a**. Only in the reaction of **I2a** was the CCSD(T) method[44] applied to calculate E_a and ΔE values, to compare these values among DFT, MP2-MP4(SDQ), and CCSD(T) methods, where we selected this reaction because the size of this system was not very large and its CCSD(T) calculation could be carried out. In CCSD(T) calculations, the contribution of triple excitations was evaluated noniteratively with the CCSD wave function.[44]

In the evaluation of E_a and ΔE values, the BS-IV system was used, where 6-311G*[45] was employed for allyl and formaldehyde moieties and a (541/541/211) set[46] was employed for valence electrons of Ru with the same ECPs as those of BS-I. The Gaussian 98 program package[47] was used for all these calculations. All the results in the tables and figures, except for Figures 1 and 6, are based on DFT/BS-IV and MP4(SDQ)/BS-IV calculations, where either DFT/BS-III or MP2/BS-III optimized geometries are adopted (see above).

Results and Discussion

Preliminary Investigation. All the reaction courses shown in Schemes 1−3 were preliminarily investigated with the MP4(SDQ)/BS-II//HF/BS-I method. In **R1a**, formaldehyde approaches the ruthenium(II) center, replacing one of the C atoms of the η^3-allyl ligand, as shown in Scheme 1A. This reaction course is called path 1a here. The allyl−aldehyde coupling reaction proceeds through two transition states, and its energy changes are shown in Figure 1A. In **R1b**, formaldehyde approaches the ruthenium(II) center either between Br and allyl ligands or between CO and allyl ligands. The former course is called path 1b, and the latter one is called path 1c (see Scheme 1). Apparently, paths 1b and 1c are more energy demanding than path 1a, as shown in Figure 1A.[48] It is noted that **Prd1a** and **Prd1c** are almost isoenergetic, while their geometries are somewhat different.

Coordination of formaldehyde with **R2a**, **R2b**, **R3a**, and **R3b** leads to formation of **I2a**, **I2b**, **I3a**, and **I3b**,

(37) Hay, P. J.; Wadt, W. R. *J. Chem. Phys.* **1985**, *82*, 299.
(38) Wadt, W. R.; Hay, P. J. *J. Chem. Phys.* **1985**, *82*, 284.
(39) Huzinaga, S.; Andzelm, J.; Klobkowski, M.; Razio-Andzelm, E.; Sakai, E.; Tatewaki, H. *Gaussian Basis Sets for Molecular Calculations*; Elsevier: Amsterdam, 1984.
(40) Dunning, T. H.; Hay, P. J. In *Methods of Electronic Structure Theory*; Schaeffer, H. F., Ed.; Plenum: New York, 1977; p 1.
(41) (a) Hehre, W. J.; Ditchfield, R.; Pople, J. A. *J. Chem. Phys.* **1972**, *56*, 2257. (b) Hariharan, P. C.; Pople, J. A. *Mol. Phys.* **1972**, *27*, 209.
(42) Beck, A. D. *Phys. Rev. A* **1988**, *38*, 3098; *J. Chem. Phys.* **1993**, *98*, 1372, and 5648.
(43) Lee, C.; Yang, W.; Parr, R. G. *Phys. Rev. B* **1988**, *37*, 785.
(44) Pople, J. A.; Head-Gordon, M.; Raghavachari, K. *J. Chem. Phys.* **1987**, *87*, 5968.
(45) Krishnan, R.; Binkley, J. S.; Pople, J. A. *J. Chem. Phys.* **1980**, *72*, 650.
(46) Couty, M.; Hall, M. B. *J. Comput. Chem.* **1996**, *17*, 1359.
(47) Frisch, M. J.; Trucks, G. W.; Schlegel, H. B.; Scuseria, G. E.; Robb, M. A.; Cheeseman, J. R.; Zakrzewski, V. G.; Montgomery, J. A., Jr.; Stratmann, R. E.; Burant, J. C.; Dapprich, S.; Millam, J. M.; Daniels, A. D.; Kudin, K. N.; Strain, M. C.; Farkas, O.; Tomasi, J.; Barone, V.; Cossi, M.; Cammi, R.; Mennucci, B.; Pomelli, C.; Adamo, C.; Clifford, S.; Ochterski, J.; Petersson, G. A.; Ayala, P. Y.; Cui, Q.; Morokuma, K.; Malick, D. K.; Rabuck, A. D.; Raghavachari, K.; Foresman, J. B.; Cioslowski, J.; Ortiz, J. V.; Stefanov, B. B.; Liu, G.; Liashenko, A.; Piskorz, P.; Komaromi, I.; Gomperts, R.; Martin, R. L.; Fox, D. J.; Keith, T.; Al-Laham, M. A.; Peng, C. Y.; Nanayakkara, A.; Gonzalez, C.; Challacombe, M.; Gill, P. M. W.; Johnson, B. G.; Chen, W.; Wong, M. W.; Andres, J. L.; Head-Gordon, M.; Replogle, E. S.; Pople, J. A. *Gaussian 98*; Gaussian, Inc.: Pittsburgh, PA, 1998.
(48) Even if the first transition state of paths 1b and 1c needed a smaller activation energy than that of path 1a, the energies to reach **TS1b#2** and **TS1c#2** are estimated to be 13.0 kcal/mol + 15.6 kcal/mol for **TS1b#2** and 13.0 kcal/mol + 8.8 kcal/mol for **TS1c#2**, respectively, where 13.0 kcal/mol is the energy difference between **R1a** and **R1b**, and 15.6 and 8.8 kcal/mol are E_a values for the second transition states **TS1b#2** and **TS1c#2**, respectively. Thus, paths 1b and 1c are more energy-demanding than path 1a.

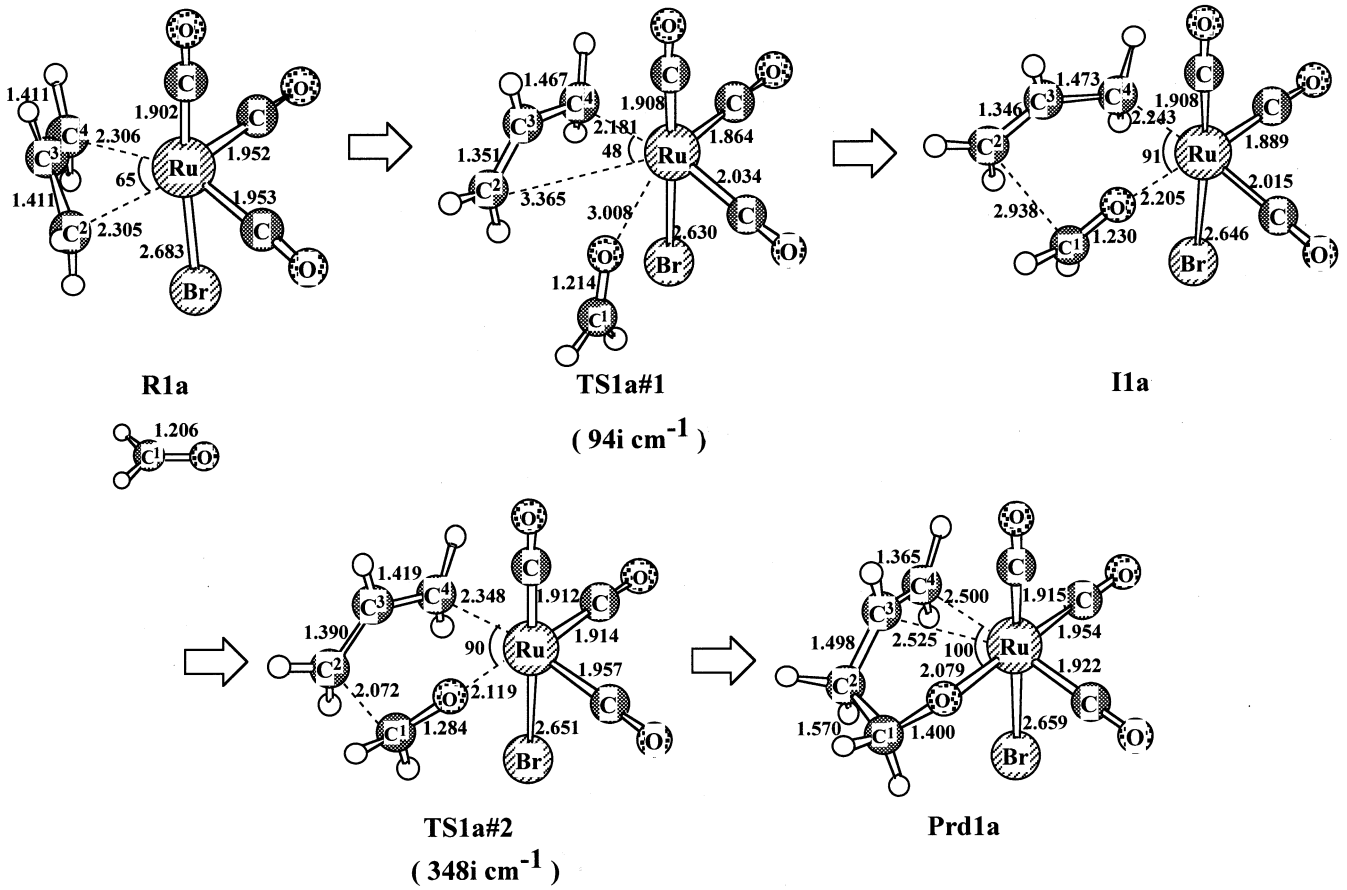

Figure 2. DFT/BS-III optimized geometry changes (bond lengths in Å and bond angles in deg) in the allyl−aldehyde coupling reaction (path 1a) with RuBr(η^3-C_3H_5)$(CO)_3$ (**R1a**). Imaginary frequencies (DFT/BS-III calculation) are given in parentheses.

respectively (vide supra), in which the allyl−aldehyde coupling reaction proceeds. Their reaction courses are defined in Schemes 2 and 3. The reaction of **I2a** (path 2a) occurs more easily than that of **I2b** (path 2b), as shown in Figure 1B. Also, **I3a** is more stable than **I3b**, and its reaction (path 3a)[49] proceeds with a lower activation barrier than that of **I3b** (path 3b) (see Figure 1C).

Considering these preliminary results, we will investigate paths 1a, 1b, and 1c in more detail in the next section.

Geometry Changes by the Coupling Reaction. In paths 1a, 2a, and 3a, geometry changes were reoptimized with either the DFT(B3LYP)/BS-III method or the MP2/BS-III method, and energy changes were evaluated with DFT(B3LYP)/BS-IV and MP4(SDQ)/BS-IV methods.

Geometry changes along path 1a are shown in Figure 2. In the first transition state, **TS1a#1**, formaldehyde approaches the ruthenium(II) center of **R1a** and the C^2 atom of the allyl group dissociates from the ruthenium(II) center, while the Ru−O distance is still very long (3.008 Å). The Ru−C^2 distance greatly lengthens to 3.365 Å and the Ru−C^4 distance considerably shortens to 2.181 Å. Consistent with these Ru−C^2 and Ru−C^4 distances, the allyl moiety in **TS1a#1** becomes similar to the η^1-allyl ligand. These features indicate that coordination of formaldehyde with the ruthenium(II) center has not been completed in this transition state, whereas the C^2 atom of the allyl group almost dissociates from the ruthenium(II) center and the allyl moiety considerably changes to the η^1-allyl form from the η^3-allyl form. These features suggest that the origin of the activation energy is the geometry change from the η^3-allyl form to the η^1-allyl form; actually, the η^1-allyl form is much less stable than the η^3-allyl form, as shown below. In the intermediate RuBr(η^1-C_3H_5)(HCHO)$(CO)_3$ (**I1a**), the Ru−O distance is 2.205 Å, which is in the range of a normal coordinate bond distance. The C^2−C^3 (1.346 Å) and C^3−C^4 (1.473 Å) distances show that the allyl group has completely changed to the η^1-allyl form from the η^3-allyl form. With **I1a** as the starting point, the allyl−aldehyde coupling reaction proceeds through the second transition state, **TS1a#2**. In this transition state, only one imaginary frequency (348i cm^{-1}) was calculated with the DFT(B3LYP)/BS-III method. The C^1−C^2 distance of 2.072 Å is much longer than the usual C−C single bond. The C^3−C^4 distance shortens to 1.419 Å and the C^2−C^3 distance lengthens to 1.390 Å in **TS1a#2**. These geometry changes are consistent with the features that the C^3−C^4 single bond converts to the C=C double bond while the C^2=C^3 double bond converts to the C−C single bond upon going to the product RuBr(OCH_2CH_2CH=CH_2)$(CO)_3$ (**Prd1a**) from **I1a**. Although the Ru−O distance (2.119 Å) of **TS1a#2** is 0.04 Å longer than that of **Prd1a** but 0.09 Å

(49) In path 3a, the different transition state structure is possible, in which the C^1 atom of formaldehyde approaches the C^4 atom of the allyl moiety. However, this transition state structure is slightly more unstable than **TS3a** by ca. 2 kcal/mol (MP4(SDQ)/BS-IV//HF/BS-III).

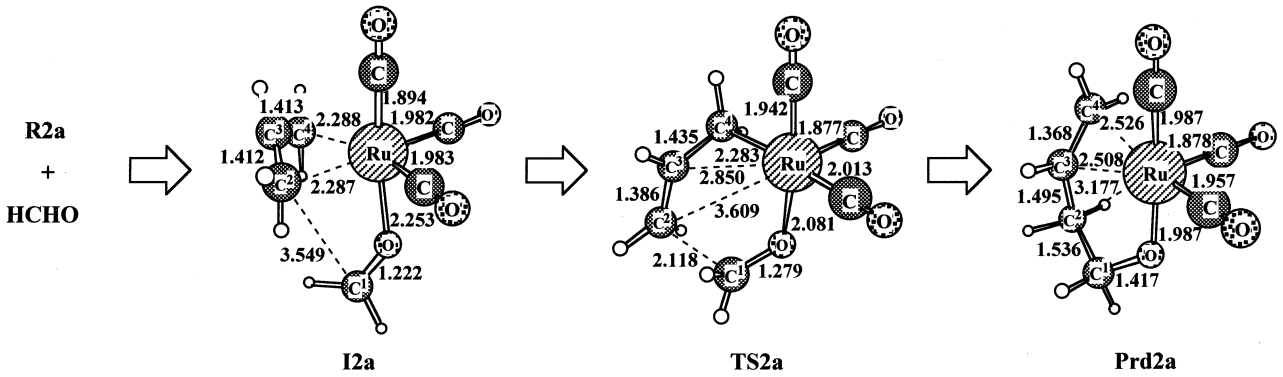

Figure 3. DFT/BS-III optimized geometry changes (bond lengths in Å and bond angles in deg) in the allyl−aldehyde coupling reaction (path 2a) with $[Ru(\eta^3\text{-}C_3H_5)(HCHO)(CO)_3]^+$ (**I2a**).

shorter than that of **I1a**, the C^1-O bond of **TS1a#2** is 0.05 Å longer than that in **I1a** but 0.12 Å shorter than that of **Prd1a**. These features indicate that the Ru−O interaction starts to change before the geometry change of the formaldehyde moiety in this **TS1a#2**. In the product **Prd1a**, the C^3-C^4 distance is 1.365 Å and the C^2-C^3 distance is 1.498 Å, which shows that the C^3-C^4 bond is a double bond and the C^2-C^3 bond is a single bond. It is noted here that the $Ru-C^3$ and $Ru-C^4$ distances (2.525 and 2.500 Å, respectively) are longer than the usual metal−carbon distances of transition-metal alkene complexes. These long distances suggest that the C=C double bond rather weakly coordinates with the ruthenium(II) center in **Prd1a**.

Figure 3 shows geometry changes in path 2a which starts from the (η^3-allyl)ruthenium(II) formaldehyde complex $[Ru(\eta^3\text{-}C_3H_5)(HCHO)(CO)_3]^+$ (**I2a**) to the product $[Ru(OCH_2CH_2CH{=}CH_2)(CO)_3]^+$ (**Prd2a**). In **I2a**, the allyl ligand takes the typical η^3-allyl form, and the Ru−O distance (2.253 Å) is somewhat longer than that of **I1a**. Since CO is at a position trans to formaldehyde in both **I1a** and **I2a**, CO is not responsible for this longer Ru−O distance in **I2a**. One important difference between **I1a** and **I2a** is that the allyl moiety takes the η^1-allyl form in **I1a** but the η^3-allyl form in **I2a**. Since the η^3-allyl ligand is more electron donating than the η^1-allyl ligand (vide infra), the η^3-allyl ligand suppresses the electron donation of formaldehyde to the ruthenium(II) center, which leads to a weaker Ru−O bond; i.e., the longer Ru−O distance in **I2a** compared to that of **I1a**. The C^1-C^2 distance (2.118 Å) of **TS2a** is much longer than the usual C−C single bond. The C^1-C^2, C^2-C^3 (1.386 Å), C^3-C^4 (1.435 Å), and Ru−O (2.081 Å) distances are similar to those of **TS1a#2**. It should be noted that the η^3-allyl ligand has become similar to the η^1-allyl form in this transition state. **Prd2a** takes a distorted-square-pyramidal structure, because Ru(II) has a d^6 electron configuration. Also, it is noted that the $Ru-C^3$ and $Ru-C^4$ distances are quite long, like those in **Prd1a**. This geometrical feature clearly shows that the C=C double bond rather weakly coordinates with the ruthenium(II) center in **Prd2a** as well.

Figure 4 shows geometry changes from the (η^3-allyl)-ruthenium(II) formaldehyde complex $RuBr(\eta^3\text{-}C_3H_5)(HCHO)(CO)_2$ (**I3a**) to the product $RuBr(OCH_2CH_2CH{=}CH_2)(CO)_2$ (**Prd3a**). Apparently, the DFT-optimized geometry of **TS3a** is significantly different from the HF-optimized one; for instance, the position of Br significantly changes in the DFT optimization, while it changes little in the HF optimization. We also reoptimized the geometries of **I3a**, **TS3a**, and **Prd3a** with the MP2/BS-III method. In the MP2-optimized **TS3a**, Br moves very little, unlike the case for the DFT-optimized transition state, whereas MP2 and DFT methods provide geometries similar to each other in **I3a** and **Prd3a**. Since Br takes a position cis to CO in **Prd3a** even in the DFT-optimized geometry, there seems no reason that Br must move in **TS3a**. Hence, we adopted the MP2-optimized geometries in path 3a. In **I3a**, the Ru−O distance (2.234 Å) is somewhat longer than that of **I1a**, like that in **I2a**. In **TS3a**, the C^1-C^2 distance is 1.984 Å, which is somewhat shorter than that in **TS1a#2**. It is noted that the C^2-C^3 bond is considerably longer than the C^3-C^4 bond. This means that the C^2-C^3 bond has almost changed to a C−C single bond in **TS3a** unlike the case in **TS1a#2** and **TS2a**, in which the C^2-C^3 bond is still characterized to be a C=C double bond; in other words, the geometry of the allyl moiety resembles the η^1-allyl form and at the same time becomes similar to that of the product. These features suggest that **TS3a** is more productlike than the others. In the product **Prd3a**, the $Ru-C^3$ and $Ru-C^4$ distances are 2.191 (2.376) Å and 2.264 (2.371) Å, respectively, where values without parentheses are MP2-optimized and values in parentheses are DFT-optimized. These distances are in the range of the usual metal−carbon distances of transition-metal alkene complexes. These geometrical features indicate that the C=C double bond more strongly coordinates with the ruthenium(II) center in **Prd3a** than those in **Prd1a** and **Prd2a**. This difference between **Prd3a** and the others is interpreted in terms of the strong trans influence of CO and the weak trans influence of Br; in **Prd3a**, Br takes a position trans to the C=C double bond, while CO takes a position trans to the C=C double bond in **Prd1a** and **Prd2a**.

As will be discussed below, path 1a is the best, probably because the six-coordinate saturated structure is favorable for the reaction. Since aldehyde exists in excess under the catalytic reaction conditions, one more formaldehyde molecule can coordinate with the ruthenium(II) center in **I2a** and **I3a**. This leads to formation of a coordinatively saturated ruthenium(II) complex. Thus, we investigated the allyl−aldehyde coupling reaction of **I2a** with one more formaldehyde molecule, where this reaction course is called path 4. We adopted

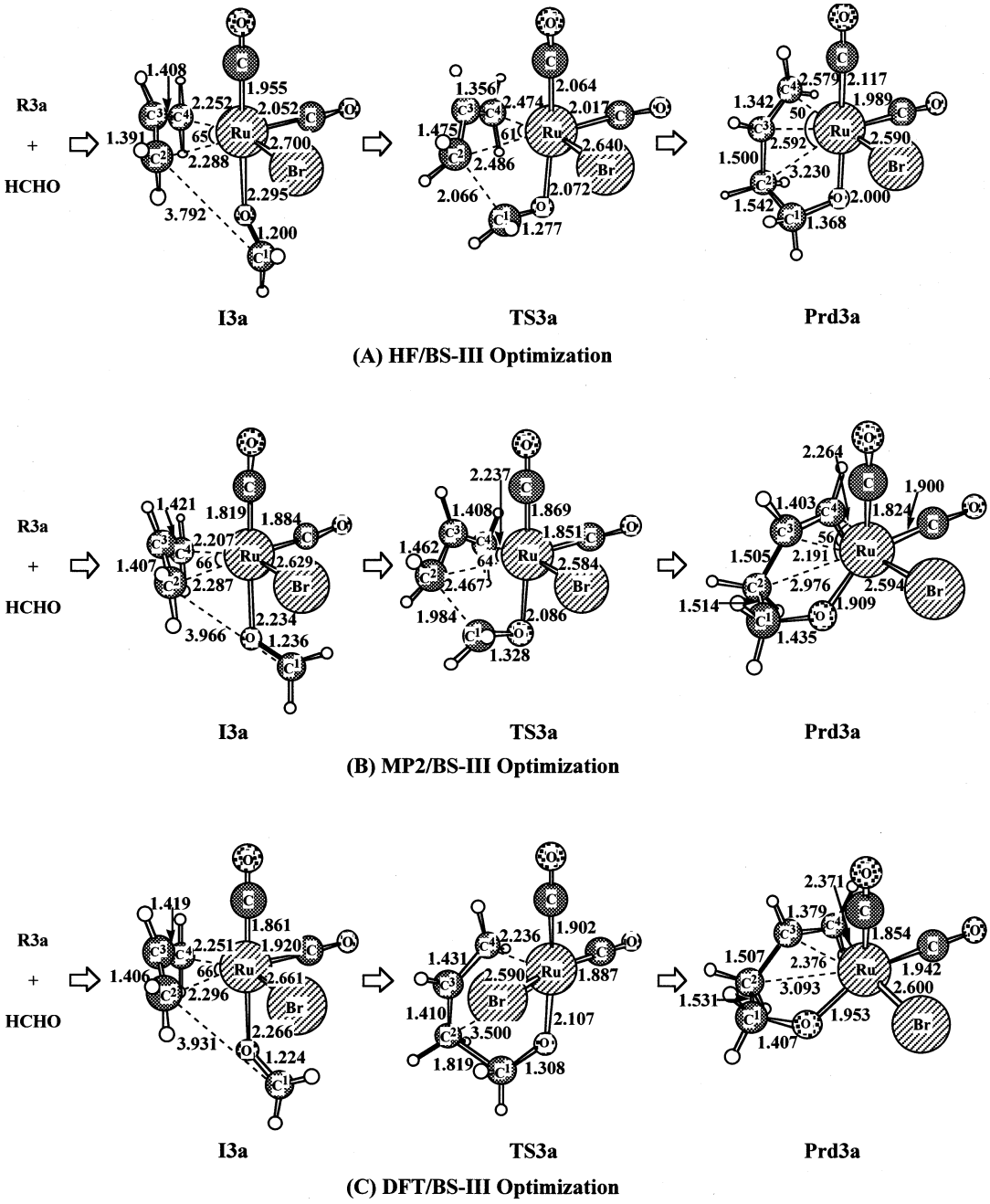

Figure 4. DFT/BS-III optimized geometry changes (bond lengths in Å and bond angles in deg) in the allyl−aldehyde coupling reaction (path 3a) with $RuBr(\eta^3\text{-}C_3H_5)(HCHO)(CO)_2$ (**I3a**).

here **I2a**, since OTf^- is considered to dissociate easily from the ruthenium(II) center of $Ru(OTf)(\eta^3\text{-}C_3H_5)(CO)_3$.[50] As shown in Figure 5, coordination of the second formaldehyde with the ruthenium(II) center occurs through the first transition state (**TS4#1**), to afford the $(\eta^1$-allyl)ruthenium(II) formaldehyde complex $[Ru(\eta^1\text{-}C_3H_5)(HCHO)_2(CO)_3]^+$ (**I4**), which is similar to **I1a**. The allyl−aldehyde coupling reaction starts from **I4** to produce the product $[Ru(OCH_2CH_2CH{=}CH_2)(HCHO)(CO)_3]^+$ (**Prd#4**) through the second transition state **TS4#2**. These geometry changes are essentially the same as those of path 1a.

Energy Changes of the Allyl−Aldehyde Coupling Reaction. In all the reaction paths, the E_a values of the DFT calculation are much smaller than those of the MP4(SDQ) calculation, as shown in Tables1 and 2. To investigate which of the DFT and MP4(SDQ) methods is more reliable, we calculated here the E_a and ΔE values of path 2a with the CCSD(T) method. The E_a value somewhat fluctuates around MP2 to MP4(DQ) levels but seems to converge upon going to MP4(SDQ). The ΔE value moderately decreases upon going to MP3 from MP2 but converges upon going to MP4(SDQ) from MP3 as well. Though the MP4(SDQ)-calculated ΔE value deviates from the CCSD(T) value to a greater extent than does the DFT value, the MP4(SDQ)-calculated

(50) CO elimination from the ruthenium(II) center occurs in general under UV-light irradiation,[34] but this allyl−aldehyde coupling reaction proceeds without UV-light irradiation. This means that the possibility of the presence of **R2** and **I2** is not large in the reaction system. On the other hand, OTf^- easily dissociates from the ruthenium(II) center. Thus, we adopted not **I3a** but **I2a** for further investigation about coordination of two molecules of formaldehyde.

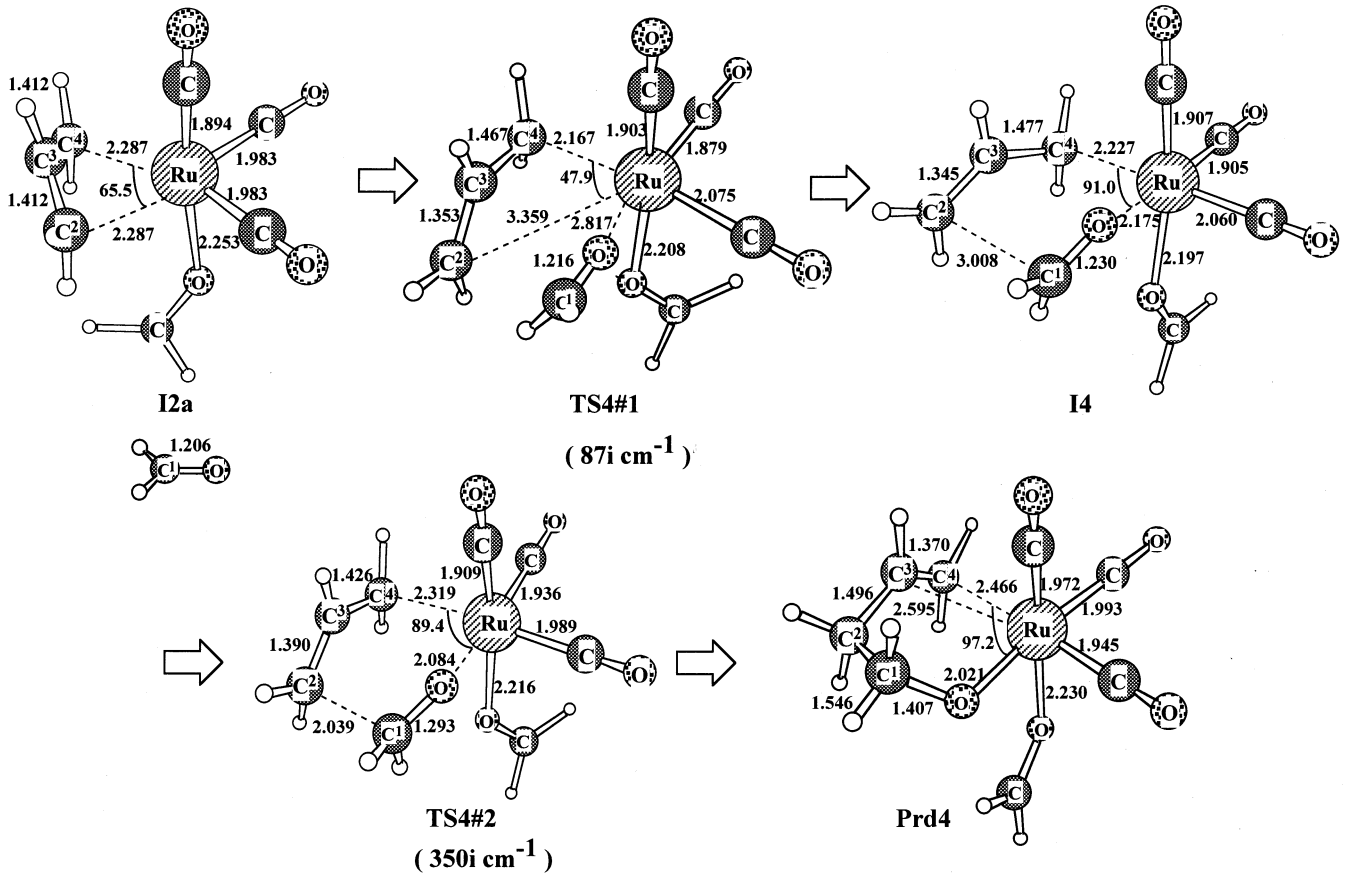

Figure 5. DFT/BS-III optimized geometry changes (bond lengths in Å and bond angles in deg) in the allyl−aldehyde coupling reaction (path 4) between $[Ru(\eta^3\text{-}C_3H_5)(HCHO)(CO)_3]^+$ (**I2a**) and HCHO. Imaginary frequencies (DFT/BS-III calculation) are given in parentheses.

Table 1. Comparisons of Activation Barriers (E_a) and Reaction Energies (ΔE) (kcal/mol) Calculated with Various Computational Methods in the Allyl−Aldehyde Coupling Reaction (Path 2a) of $[Ru(\eta^3\text{-}C_3H_5)(HCHO)(CO)_3]^+$

	E_a[a]	ΔE[b]		E_a[a]	ΔE[b]
DFT	30.6	17.1	MP4(SDQ)	50.7	33.1
MP2	47.9	37.0	CCSD	50.8	25.3
MP3	51.7	34.1	CCSD(T)	46.4	24.7
MP4(DQ)	54.6	34.1			

[a] Energy difference between transition state and reactant. [b] Energy difference between product and reactant.

E_a value deviates from the CCSD(T) value to a lesser extent than does the DFT value. From these results, it is not easy to determine which of the DFT and MP4(SDQ) methods is the more reliable here. Thus, we will present our discussion based on both DFT and MP4(SDQ) methods.

Energy changes of paths 1a, 2a, 3a, and 4 calculated with DFT/BS-IV and MP4(SDQ)/BS-IV methods are listed in Table 2, where geometries optimized with the DFT(B3LYP)/BS-III method were adopted in paths 1a, 2a, and 4 but those optimized with the MP2/BS-III method were adopted in path 3a (vide supra). In path 1a, it is noted that **I1a** is somewhat less stable than **R1a** (see Table 2A). This result means that the η^3-allyl ligand forms a stronger bonding interaction with the ruthenium(II) center than does the η^1-allyl ligand. The E_a value is 19.9 (12.0) kcal/mol for the first transition state and 12.5 (5.4) kcal/mol for the second transition state, where MP4(SDQ)-calculated E_a values are given

Table 2. Energy Changes in Allyl−Aldehyde Coupling Reactions with (η^3-Allyl)ruthenium(II) Complexes

(A) $RuBr(\eta^3\text{-}C_3H_5)(CO)_3$ (**R1a**) + HCHO → $RuBr(OCH_2CH_2CH{=}CH_2)(CO)_3$ (**Prd1a**) (Path 1a)[a]

	R1a	TS1a#1	I1a	TS1a#2	Prd1a
DFT	0.0	12.0	2.6	8.0	−3.1
MP4(SDQ)	0.0	19.9	10.5	23.0	3.4

(B) $[Ru(\eta^3\text{-}C_3H_5)(HCHO)(CO)_3]^+$ (**I2a**) → $[Ru(OCH_2CH_2CH{=}CH_2)(CO)_3]^+$ (**Prd2a**) (Path 2a)[a,b]

	I2a	TS2a	Prd2a
DFT	0.0	30.6	17.1
MP4(SDQ)	0.0	50.7	34.1

(C) $RuBr(\eta^3\text{-}C_3H_5)(HCHO)(CO)_2$ (**I3a**) → $RuBr(OCH_2CH_2CH{=}CH_2)(CO)_2$ (**Prd3a**) (Path 3a)[b,c]

	I3a	TS3a	Prd3a
DFT	0.0	32.0	5.2
MP4(SDQ)	0.0	34.8	7.8

(D) $[Ru(\eta^3\text{-}C_3H_5)(HCHO)(CO)_3]^+$ (**I2**) + HCHO → $[Ru(OCH_2CH_2CH{=}CH_2)(CO)_3(HCHO)]^+$ (**Prd4**) (Path 4)[a]

	I4	TS4#1	I4	TS4#2	Prd4
DFT	0.0	12.0	2.6	8.0	−3.1
MP4(SDQ)	0.0	19.9	10.5	23.0	3.4

[a] DFT-optimized geometries. [b] **I2a** and **I3a** are taken to be the standard (energy 0), since a transition state was not found between **I2a** and **R2a** and between **I3a** and **R3a**. [c] MP2-optimized geometries.

without parentheses and DFT-calculated values are given in parentheses hereafter. Apparently, these E_a values are moderate and the path 1a is much less endothermic than paths 2a and 3a. In paths 2a and 3a, the E_a value is significantly large and the reaction is considerably endothermic (parts B and C of Table 2). In path 4, the E_a value is 10.5 (4.6) kcal/mol for the first transition state and 12.6 (6.7) kcal/mol for the second transition state (part D of Table 2). These results lead us to the following conclusions: (1) a coordinatively saturated complex, RuBr(η^3-C_3H_5)$(CO)_3$, is reactive for the allyl−aldehyde coupling reaction, (2) coordinatively unsaturated complexes, [Ru(η^3-C_3H_5)$(CO)_3$]$^+$ and RuBr(η^3-C_3H_5)$(CO)_2$, are not reactive for this reaction, when only one formaldehyde reacts with them, and (3) [Ru(η^3-C_3H_5)(HCHO)$(CO)_3$]$^+$ becomes reactive for this reaction, when one more formaldehyde molecule coordinates with the ruthenium(II) center. These conclusions are consistent with the experimental result that both Ru(OTf)(η^3-C_3H_5)$(CO)_3$ and RuBr(η^3-C_3H_5)$(CO)_3$ provide considerably large yields of homoallyl alcohol in the allyl−aldehyde coupling reaction[3b] (remember that OTf^- would easily dissociate from the ruthenium(II) center and dissociation of OTf^- followed by coordination of formaldehyde leads to [Ru(η^3-C_3H_5)(HCHO)$(CO)_3$]$^+$).

Electronic Process of the Allyl−Aldehyde Coupling Reaction. In path 1a, the IRC calculation[51] was carried out with the HF/BS-I method. Though the HF-optimized transition state structure is somewhat different from the DFT-optimized one, the position of the transition state on the reaction coordinate is almost the same in both MP4(SDQ)/BS-II//HF/BS-I and HF/BS-I calculations, as shown in Figure 6. From this result, the IRC calculation with the HF/BS-I method seems meaningful. Several important geometrical parameters are plotted against the reaction coordinate in the lower half of Figure 6. The C^1-C^2 distance starts to shorten at an early stage of the reaction, while the C^2-C^3 bond starts to lengthen and the C^3-C^4 bond starts to shorten later than the C^1-C^2 distance changes. The C^2-C^3 and C^3-C^4 bond distances cross toward each other at a stage later than the transition state. At this position, the C^1-C^2 distance is about 1.8 Å, indicating that the C−C bond formation effectively occurs around here. This means that the C^1-C^2 bond is formed concomitantly with the bond alternation in the allyl moiety after the transition state. The C^1-O distance lengthens in the reaction because the $C^1=O$ double bond of aldehyde changes into a C^1-O single bond in the product. This bond lengthening occurs moderately before the transition state but substantially after the transition state. These results suggest that the transition state is rather reactant-like and the electronic structure of the ruthenium complex changes after the transition state.

Electron redistribution by the reaction also provides us valuable information about the electronic process. Changes of natural bond orbital (NBO)[52] charges are shown in Figure 7. In path 1a, the positive charge of formaldehyde increases but that of the allyl moiety decreases upon going to **I1a** from **R1a**. These results clearly show that the η^3-allyl ligand is more electron-donating than the η^1-allyl ligand and that formaldehyde donates its lone pair electrons to the ruthenium(II) center. The conversion from **I1a** to **Prd1a** induces a different kind of electron redistribution; for instance, the positive charge of formaldehyde decreases and the allyl moiety becomes positively charged upon going from **I1a** to **Prd1a**. Since the conversion from **I1a** to **Prd1a** involves C−C bond formation between allyl and formaldehyde, it is reasonably concluded that the charge transfer from the η^1-allyl ligand to formaldehyde takes place in the C−C bond formation; in other words, the allyl−aldehyde coupling reaction is understood in terms of an electrophilic attack of formaldehyde at the C=C double bond of the allyl moiety. The Ru atomic charge does not change very much during the reaction. Consistent with the electron redistribution described above, the C^1 positive charge decreases and the O negative charge increases upon going to **Prd1a** from **I1a**, while C^3 and C^4 negative charges decrease. However, the C^2 negative charge increases, which is in contrast to the expectation from the charge transfer from the η^1-allyl ligand to formaldehyde. These changes suggest that not only the charge transfer from the η^1-allyl ligand to formaldehyde but also the polarization occurs in the η^1-allyl moiety, as shown in Chart 1. A similar electron redistribution is observed in path 4 (see ref 53 and the

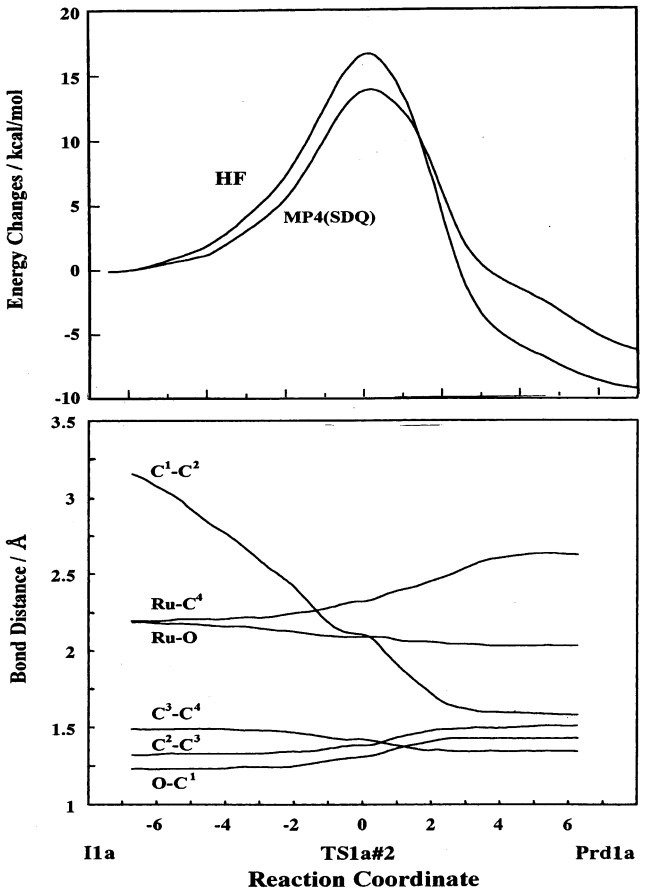

Figure 6. Results of IRC calculations (HF/BS-I) of the allyl−aldehyde coupling reaction from RuBr(η^1-C_3H_5)$(CO)_3$ (**I1a**) to RuBr($OCH_2CH_2CH{=}CH_2$)$(CO)_3$ (**Prd1a**).

(51) Fukui, K. *Acc. Chem. Res.* **1981**, *14*, 363 and references therein.
(52) (a) Reed, A. E.; Weinstock, R. B.; Weinhold, F. *J. Chem. Phys.* **1985**, *83*, 735. (b) Reed, A. E.; Curtis, L. A.; Weinhold, F. *Chem. Rev.* **1988**, *88*, 899 and references therein.
(53) Only one difference in electron redistribution between path 1a and path 4 is that formaldehyde of a spectator ligand is positively charged in path 4 but Br is negatively charged in the path 1a. However, both NBO charges change little in the reaction.

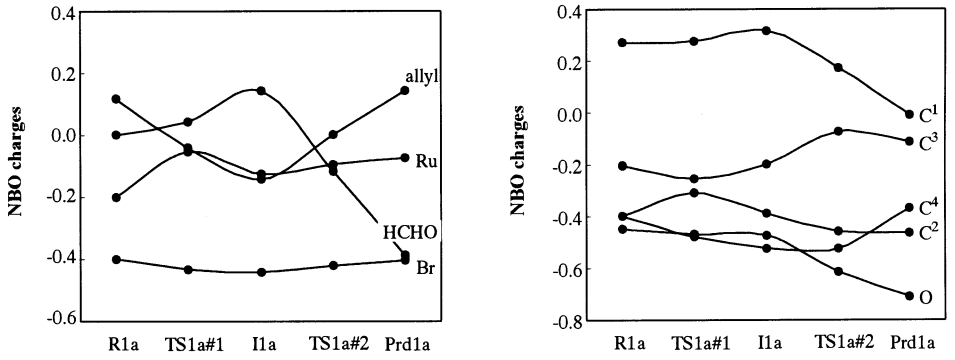

(A) $RuBr(\eta^3\text{-}C_3H_5)(CO)_3 + HCHO$

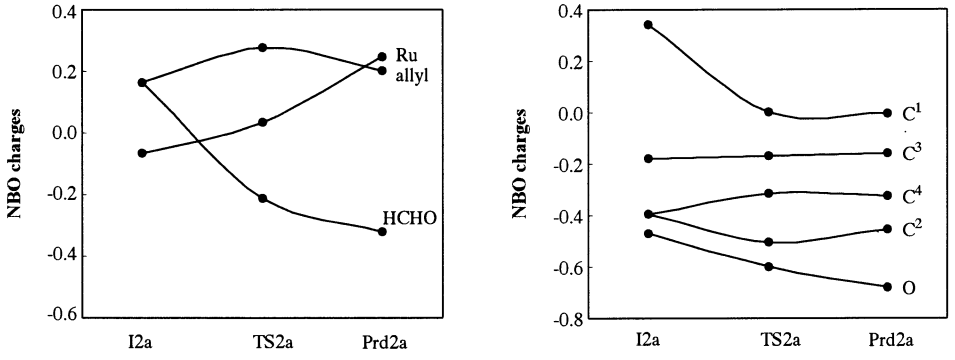

(B) $[Ru(\eta^3\text{-}C_3H_5)(CO)_3]^+ + HCHO$

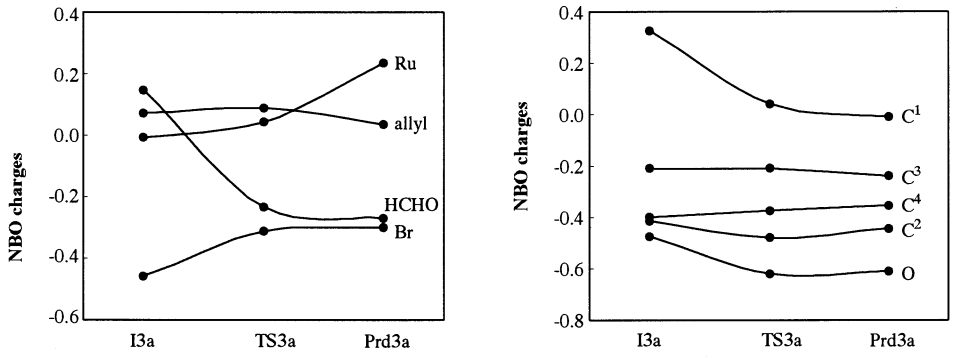

(C) $RuBr(\eta^3\text{-}C_3H_5)(CO)_2 + HCHO$

Figure 7. Changes in MP4(SDQ)/BS-IV calculated NBO charges by the allyl−aldehyde coupling reactions with $RuBr(\eta^3\text{-}C_3H_5)(CO)_3$ (**R1a**), $[Ru(\eta^3\text{-}C_3H_5)(HCHO)(CO)_3]^+$ (**I2a**), and $RuBr(\eta^3\text{-}C_3H_5)(HCHO)(CO)_2$ (**13a**).

Chart 1

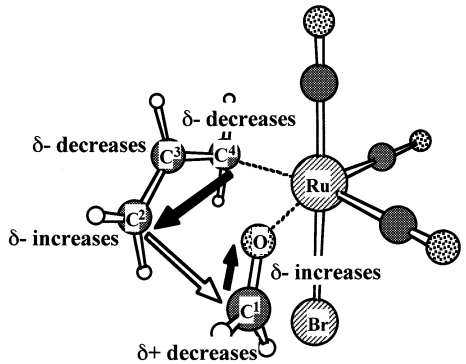

⇨ CT = Electron flow by charge-transfer

➡ Pol = Electron flow by polarization

Supporting Information). All these geometry changes and electron redistributions correspond to the reaction feature shown in Chart 2. This reaction feature and the

Chart 2

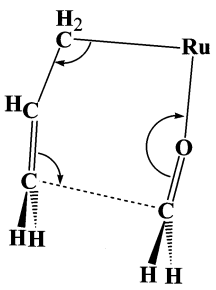

transition state structure are consistent with the six-centered transition state that was experimentally pro-

posed for the Sn-promoted allyl−aldehyde coupling reaction.[10,54]

Electron redistributions in paths 2a and 3a are shown in parts B and C, respectively, of Figure 7. The positive charge of formaldehyde decreases in these reactions, similar to that in path 1a. However, the positive charge of the allyl moiety changes little but the Ru positive charge considerably increases, in contrast to the case for path 1a. These features suggest that formaldehyde receives electrons from the allyl moiety and at the same time the allyl moiety is provided electrons by the ruthenium(II) center. These features are deeply related to the large E_a values of paths 2a and 3a, which will be discussed below in detail.

Reasons That [RuBr(η^3-C_3H_5)$(CO)_3$] and [Ru(η^3-C_3H_5)(HCHO)$(CO)_3$]$^+$ Are More Reactive Than [Ru(η^3-C_3H_5)$(CO)_3$]$^+$ and [RuBr(η^3-C_3H_5)$(CO)_2$] in the Allyl−Aldehyde Coupling Reaction. It is important to clarify the reasons that the allyl−aldehyde coupling reaction proceeds more easily in paths 1a and 4 than in paths 2a and 3a. This coupling reaction contains two processes; one is the conversion of the η^3-allyl form to the η^1-allyl form, and the other is the C−C bond formation between η^1-allyl and formaldehyde ligands. In paths 1a and 4, the η^3-allyl form converts to the η^1-allyl form concomitantly with coordination of formaldehyde to the ruthenium(II) center upon going to RuBr(η^1-C_3H_5)(HCHO)$(CO)_3$ and [Ru(η^1-C_3H_5)$(HCHO)_2$-$(CO)_3$]$^+$ from RuBr(η^3-C_3H_5)$(CO)_3$ and [Ru(η^3-C_3H_5)-(HCHO)$(CO)_3$]$^+$, respectively. In general, the η^3-allyl form is much more stable than the η^1-allyl form,[31] and actually, RuBr(η^3-C_3H_5)$(CO)_3$ is 51 kcal/mol more stable than RuBr(η^1-C_3H_5)$(CO)_3$ (MP4(SDQ)/BS-II//HF/BS-I), where the C=C double bond of the η^1-allyl moiety is placed at the most distant position from the ruthenium(II) center. However, [RuBr(η^1-C_3H_5)(HCHO)$(CO)_3$] is about 10.5 (2.6) kcal/mol less stable than [RuBr(η^3-C_3H_5)$(CO)_3$] + HCHO, and [Ru(η^1-C_3H_5)$(HCHO)_2(CO)_3$]$^+$ is about 2.3 (−3.6) kcal/mol less stable than [Ru(η^3-C_3H_5)(HCHO)$(CO)_3$]$^+$ + HCHO. Thus, the destabilization caused by the conversion of the η^3-allyl form to the η^1-allyl form would be mostly compensated by the coordination of formaldehyde to the ruthenium(II) center. After this conversion, a C−C bond is formed between the η^1-allyl ligand and formaldehyde. Though the activation energy is also necessary for this process, it is not very large, since the geometry of the η^1-allyl ligand resembles that of the allyl moiety in **TS1a#2** and **TS4#2**. In paths 2a and 3a, formaldehyde easily coordinates with the ruthenium(II) center to afford **I2a** and **I3a**, in which the η^3-allyl form is still maintained; in other words, the C−C bond formation occurs concomitantly with the significantly large geometry changes from the η^3-allyl form to the η^1-allyl one. Thus, the activation energy is necessary for these two processes at one time. This would be the main reason that paths 2a and 3a need greater E_a values than paths 1a and 4.

The electron distribution is also reflected in the reason that the reaction occurs more easily in paths 1a and 4 than in paths 2a and 3a. As shown in Figure 7A, the η^1-allyl ligand is negatively charged in **I1a**, while the η^3-allyl ligand is positively charged in **R1a** because of the strong electron-donating ability of the η^3-allyl ligand. Thus, the charge transfer from the η^1-allyl ligand to formaldehyde easily occurs in the allyl−aldehyde coupling reactions of **I1a** and **I4**.[55] In **I2a** and **I3a**, on the other hand, the η^3-allyl form is still maintained, and it directly undergoes a coupling reaction with formaldehyde. Since the η^3-allyl ligand is positively charged in **I2a** and **I3a** (see parts B and C of Figure 7), the charge transfer from the η^3-allyl ligand to formaldehyde occurs in **I2a** and **I3a** to a lesser extent than that in **I1a** and **I4**, which results in lower reactivities of **I2a** and **I3a**. In these reaction systems, the Ru positive charge increases (vide supra). This increase is also understood as follows: in **I2a** and **I3a**, C−C bond formation occurs with concomitant conversion of the η^3-allyl form to the η^1-allyl form in one step, as discussed above. The latter process increases the positive charge of the ruthenium(II) center but decreases the positive charge of the allyl ligand, since the η^3-allyl ligand is more electron donating than the η^1-allyl ligand. In the C−C bond formation, the charge transfer occurs from the allyl ligand to formaldehyde, at which point the positive charge of the allyl moiety increases and that of formaldehyde decreases. Thus, the C−C bond formation and the conversion of the η^3-allyl form to the η^1-allyl one induce reverse electron redistribution in the allyl moiety to each other. Consequently, the negative charge of the allyl moiety changes little, while the positive charge of the ruthenium(II) center increases in the reactions of **I2a** and **I3a**. In other words, two kinds of electron redistributions occur at one time in these reactions; one is the charge transfer from the allyl ligand to aldehyde, and the other is the weakening of electron donation from the allyl ligand to the ruthenium(II) center. These results indicate that the electronic structure changes in the ruthenium(II) center, allyl, and formaldehyde moieties at one time in paths 2a and 3a, which would be related to their E_a values being larger than those of paths 1a and 4.

C−C Bond Cleavage by the Ruthenium(II) Complex. The reverse reaction of the allyl−aldehyde coupling reaction corresponds to the C−C bond cleavage of homoallyl alcohol by a ruthenium(II) complex.[22] In this reaction, the (η^3-allyl)ruthenium(II) complex is formed as a product.

In the systems examined here, the best is [Ru(OCH_2-CH_2CH=CH_2)$(CO)_3$]$^+$ and the next best is RuBr(OCH_2-CH_2CH=CH_2)$(CO)_3$ for this reaction, as follows: C−C bond cleavage occurs with moderate E_a values of 19.6 (11.1) and 16.6 (13.5) kcal/mol in RuBr(OCH_2CH_2-CH=CH_2)$(CO)_3$ and [Ru(OCH_2CH_2CH=CH_2)$(CO)_3$]$^+$, respectively, but with a large E_a value of 27.0 (27.8) and 28.7 (21.2) kcal/mol in RuBr(OCH_2CH_2CH=CH_2)$(CO)_2$ and [Ru(OCH_2CH_2CH=CH_2)$(CO)_3$(HCHO)]$^+$, respectively (see Table 2). These results are interpreted in terms of the stability of the (η^3-allyl)ruthenium(II) complex. As shown in Figure 7, the η^3-allyl ligand of **I2a** is the most positively charged in these (η^3-allyl)-

(54) (a) Nokami, J.; Yoshizane, K.; Matsuura, H.; Sumida, S. *J. Am. Chem. Soc.* **1998**, *120*, 6609. (b) Sumida, J.; Ohga, M.; Mitani, J.; Nokami, J. *J. Am. Chem. Soc.* **2000**, *122*, 1310.

(55) The η^1-allyl moiety is negatively charged in **I4** as well(see the Supporting Information).

ruthenium(II) complexes, which clearly shows that the charge transfer from the η^3-allyl ligand to the ruthenium(II) center occurs to the greatest extent in **I2a**. This means that **I2a** possesses the strongest bonding interaction between the η^3-allyl ligand and the ruthenium(II) center in these (η^3-allyl)ruthenium(II) complexes. This strongest interaction of **I2a** is reasonably interpreted in terms that **I2a** possesses three CO ligands but does not have an anionic Br ligand**.** On the other hand, **I3a** possesses two CO ligands and one anionic Br ligand. Since the anionic ligand pushes up the d orbital in energy and CO stabilizes the d orbital in energy through a π-back-donating interaction, the ruthenium(II) center is more electron-accepting in **I2a** than in **I3a** and, therefore, the bonding interaction of the η^3-allyl ligand with the ruthenium(II) center is stronger in **I2a** than in **I3a**. Though the C−C bond cleavage occurs with a moderate E_a value in $RuBr(OCH_2CH_2CH{=}CH_2)(CO)_3$, this reaction is much less exothermic than that of $[Ru(OCH_2CH_2CH{=}CH_2)(CO)_3]^+$. Thus, $RuBr(OCH_2CH_2CH{=}CH_2)(CO)_3$ is inferior to $[Ru(OCH_2CH_2CH{=}CH_2)(CO)_3]^+$. This is interpreted as follows: in the final product $RuBr(\eta^3\text{-}C_3H_5)(CO)_3$, charge transfer from the η^3-allyl ligand to the ruthenium(II) center is suppressed by the Br ligand and formaldehyde must be eliminated to provide two coordination sites to the η^3-allyl ligand, which leads to loss of stabilization energy by formaldehyde coordination (note that such energy loss does not occur in the C−C bond cleavage of $[Ru(OCH_2CH_2CH{=}CH_2)(CO)_3]^+$). From the above discussion, it is reasonably predicted that a coordinatively unsaturated ruthenium(II) complex with electron-accepting ligands is considered favorable for the C−C bond cleavage.

Here, we will compare these computational results with the experimental facts reported in Ru-catalyzed C−C bond cleavage of homoallyl alcohol.[22,56] In this experiment, $RuCl_2(PPh_3)_3$ was used as a catalyst. However, we must note that the C−C bond cleavage was successfully performed under a CO atmosphere. As discussed above, CO is considered as a favorable ligand. This would be one of the reasons that the CO atmosphere is indispensable for the reaction. Actually, CO was considered to play the role of a π-acid in the experimental work.[22]

Conclusions

In this work, the allyl−aldehyde coupling reaction catalyzed by the ruthenium(II) complex was theoretically investigated with ab initio MP2-MP4(SDQ), CCSD(T), and DFT methods. Three kinds of (η^3-allyl)ruthenium(II) complexes, $RuBr(\eta^3\text{-}C_3H_5)(CO)_3$ (**R1a**), $[Ru(\eta^3\text{-}C_3H_5)(HCHO)(CO)_3]^+$ (**I2a**), and $RuBr(\eta^3\text{-}C_3H_5)(HCHO)(CO)_2$ (**I3a**), were examined. Theoretical calculations clearly show the following conclusions: (1) **R1a** is reactive for the allyl−aldehyde coupling reaction, (2) **I2a** and **I3a** are not reactive for the coupling reaction, when one more formaldehyde molecule does not interact with the ruthenium(II) center, and (3) **I2a** becomes reactive, when one more formaldehyde molecule coordinates with the ruthenium(II) center to form $[Ru(\eta^1\text{-}C_3H_5)(HCHO)_2(CO)_3]^+$ (**I4**). **I3a** is also expected to become reactive when one more formaldehyde molecule interacts with the ruthenium(II) center.

Their results are easily interpreted in terms of reaction behavior, as follows: in **R1a**, coordination of formaldehyde induces the conversion of the η^3-allyl complex **R1a** to the η^1-allyl complex $RuBr(\eta^1\text{-}C_3H_5)(CO)_3(HCHO)$ (**I1a**), and then C−C bond formation between the η^1-allyl ligand and formaldehyde occurs in the next step. In the first step, the conversion of the η^3-allyl form to the η^1-allyl form occurs to give rise to the energy destabilization, but the coordination of formaldehyde with the ruthenium(II) center mostly compensates for the energy destabilization. Hence, the activation energy is necessary only for the C−C bond formation between the η^1-allyl ligand and formaldehyde in the second step. In **I2a** and **I3a**, the η^3-allyl ligand is still maintained, and C−C bond formation between the formaldehyde and η^3-allyl ligands occurs through one transition state. This means that C−C bond formation between the allyl ligand and formaldehyde occurs with a significantly large geometry change of the η^3-allyl ligand. As a result, the activation energy is necessary for these two processes, the conversion of η^3-allyl to η^1-allyl and C−C bond formation, at one time. Thus, **I2a** and **I3a** are much less reactive than **R1a**. However, when one more formaldehyde molecule coordinates with the ruthenium(II) center in **I2a** (and probably in **I3a** as well), the (η^1-allyl)ruthenium(II) formaldehyde complex **I4** is formed, in which the allyl−aldehyde coupling reaction occurs easily, like that in **R1a**. This suggests that aldehyde should be used in high concentration when the coordinatively unsaturated (η^3-allyl)ruthenium(II) complex is applied to the allyl−aldehyde coupling reaction.

It is noted that the positive charge of the allyl moiety increases but that of aldehyde decreases upon going to the product **Prd1a** from **I1a**. These results clearly indicate that the coupling reaction is understood in terms of the electrophilic attack of aldehyde to the allyl ligand. In the reactions of **I2a** and **I3a**, the positive charge of aldehyde decreases in the reaction, while the positive charge of the allyl moiety does not change so much but the Ru positive charge increases. This is interpreted in terms of the C−C bond formation occurring concomitantly with the conversion of the η^3-allyl form to the η^1-allyl form in the reactions of **I2a** and **I3a**.

In the C−C bond cleavage of homoallyl alcohol, the driving force is considered to be the formation of a stable (η^3-allyl)ruthenium(II) complex. Since the η^3-allyl ligand is strongly electron-donating, it is suggested that an electron-accepting ruthenium(II) complex is favorable to form a stable (η^3-allyl)ruthenium(II) complex. Since CO stabilizes the d orbital in energy through the π-back-donating interaction but an anionic ligand pushes up the d orbital in energy, the ruthenium(II) center is more electron-accepting in $[Ru(OCH_2CH_2CH{=}CH_2)(CO)_3]^+$ than in $RuBr(OCH_2CH_2CH{=}CH_2)(CO)_2$. Actually, the

(56) Some differences exist between the experimentally proposed species and the present models; for instance, the $CH_2{=}CHCH_2CH_2O{-}Ru{-}H$ species was postulated in the experiment,[22] while the H (hydride) ligand was not involved in the ruthenium(II) complex investigated here. However, it is reasonably expected that meaningful conclusions concerning coexisting ligand such as CO can be presented.

C−C bond cleavage occurs in $[Ru(OCH_2CH_2CH{=}CH_2)(CO)_3]^+$ with a much smaller E_a value than that in $RuBr(OCH_2CH_2CH{=}CH_2)(CO)_2$ and with much larger exothermicity than that in $RuBr(OCH_2CH_2CH{=}CH_2)(CO)_3$. From the above discussion, one can predict that the electron-donating ligand should be used when the ruthenium(II) complexes are applied to the allyl−aldehyde coupling reaction and that the electron-accepting ligand should be used when the ruthenium(II) complexes are applied to the C−C bond cleavage. The other important point is the coordination site. In the allyl−aldehyde coupling reaction, a coordinatively saturated (η^3-allyl)ruthenium(II) complex is favorable, since the η^3-allyl form converts to the η^1-allyl form by the coordination of aldehyde and the η^1-allyl form is more reactive for the C−C bond formation than the η^3-allyl form. In the C−C bond cleavage, on the other hand, a coordinatively unsaturated ruthenium(II) complex is favorable, since the η^3-allyl ligand needs two coordination sites in the product.

Acknowledgment. S.S. thanks the reviewer for the instructive suggestion about path 4. Computations were carried out with an NEC SX5 computer at the Institute for Molecular Science (Okazaki, Japan) and a Deck Alpha Station DS20E at our laboratory. This work was supported financially in part by the Ministry of Education, Culture, Sports, and Science through Grants-in-Aid for Priority Area "Molecular Physical Chemistry (No. 403)". Also, T.K. thanks the Mitsubishi Chemical Corporation Fund for providing financial support.

Supporting Information Available: Figures giving HF/BS-I optimized geometry changes of the allyl−aldehyde coupling reactions of $RuBr(\eta^3\text{-}C_3H_5)(CO)_3$, $[Ru(\eta^3\text{-}C_3H_5)(CO)_3]^+$, and $RuBr(\eta^3\text{-}C_3H_5)(CO)_2$, and population changes of path 4. This material is available free of charge via the Internet at http://pubs.acs.org.

OM010011G